

F. Méot, CEA DAPNIA

Tracking study in Carol/Shane's PAC05 lattice

1 Fields and cell parameters

Hypothesis, geometry

The design hypothesis are, a qf-o-DD-O-qf cell. The magnets are straight multipoles with dB/dx gradient. Their axis are at an angle of $360/42/2$ degrees. The positionning of the magnets includes the following shifts : the axis of both qf magnets intersect the respectively entrance and exit of DD at a distance $\Delta x = 0.8824$ mm from DD axis toward ring center.

In the case of sharp edge field models, the first order effect of fringe field extent g on vertical focusing is accounted for via a kick with value $-\tan(\alpha)/\rho + g/(6 * \rho^2 * \cos(\alpha))$ with ρ being the local curvature and α the angle the particle makes with the magnet edge. This is to compensate the absence of tracking in B_s component in the absence of fringe fields.

The case of fringe field is discussed below.

Fields

The simulation of the rectangular dependence $B(x)$ in QF and DD uses a classical multipole modelling of the form

$$\vec{B}_n = \vec{\text{grad}}V_n \text{ with } V_n(s, x, z) = (n!)^2 \sum_{q=0}^{\infty} \frac{(-)^q G^{(2q)}(s)(x^2 + z^2)^q}{4^q q!(n+q)!} \times \sum_{m=0}^n \frac{\sin\left(\frac{m\pi}{2}\right) x^{n-m} z^m}{m!(n-m)!} \quad (1)$$

with the Henge's field fall-off model

$$G(s) = \frac{G_0}{1 + \exp\left(\sum_{i=0}^5 C_i (d(s)/g)^i\right)}$$

wherein $d(s)$ is the distance to the effective field boundary (the magnet edge), g is a scaling factor of the order of the gap size which determines the fringe field extent, and the C_i are adjustable coefficients that determine the shape of the fringe field.

The corresponding Zgoubi data file is given in App. A.

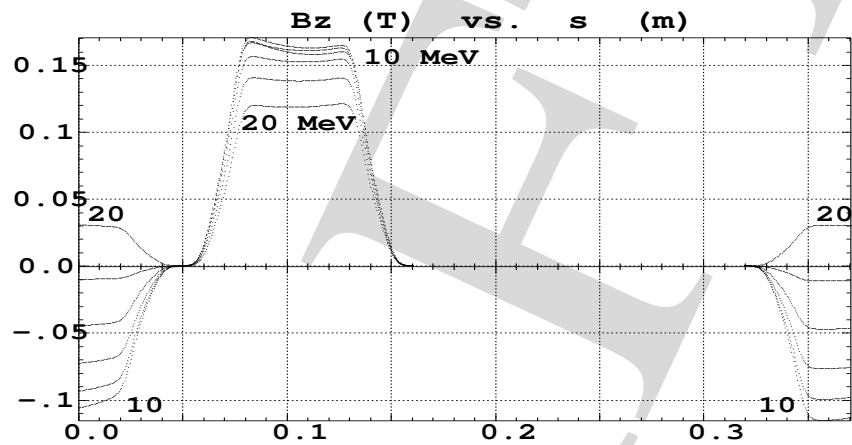


Figure 1: Field on closed orbits along the cell, at various energies. The Henge coefficients are : $C_0 = 0.1455$, $C_1 = 2.2670$, $C_2 = -0.6395$, $C_3 = 1.1558$, $C_4 = C_5 = 0$, whereas $g = 1.1$ cm.

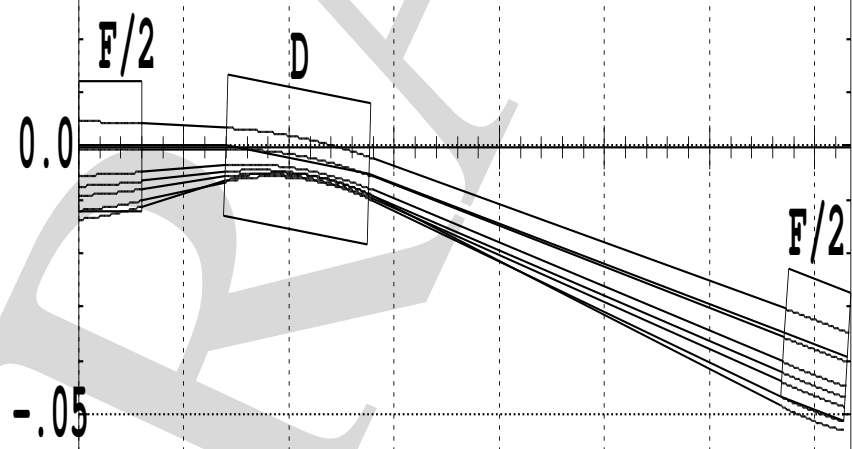


Figure 2: Closed orbits along the cell, at various energies.

2 Stability limits

Fig. 3 shows the limit horizontal phase space trajectories at various energies, in case of pure horizontal motion, or including quasi-zero z motion, which substantially decreases the DA. The fact that all these invariants are very thin gives confidence in the symplectic behavior of the integration. In particular, an increase of initial particle position by about a % results in the particle being kicked off, no fuzzy motion can be observed in the present lattice.

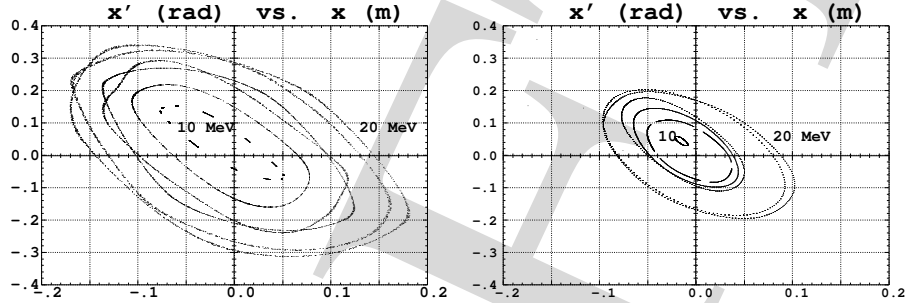


Figure 3: 2-D motion (x, x'), 1000-cell stability limits, at about % precision in x , at 10, 12, 14, 16, 18 and 20 MeV (respectively from the inner to the outer invariant on both graphs). Fringe fields are set. Left : case of pure horizontal motion (Note : practically the same figure is obtained with sharp edge model). Right : in presence of very small z motion ; one observes that introducing a z component strongly affects the DA.

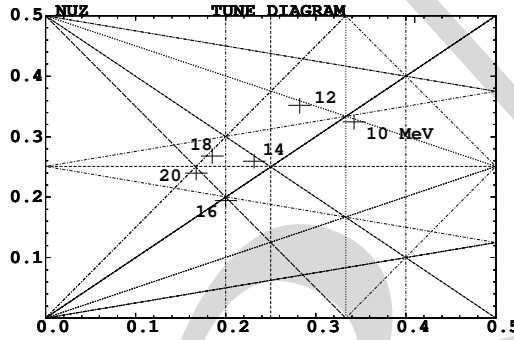


Figure 4: Cell tunes at stability limits, coupled x-z case as shown in Fig. 3-right. Resonance lines are represented up to 5th order.

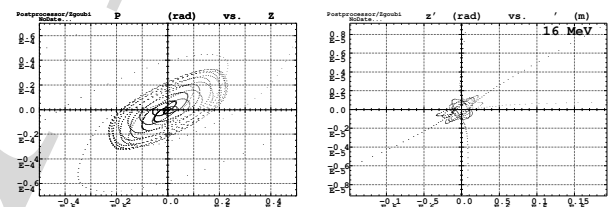


Figure 5: Vertical motion of the 10 (first plot) and 16 MeV (second) particles shown in Fig. 3. They are “extracted” on respectively a 3rd and a 5th integer resonance.

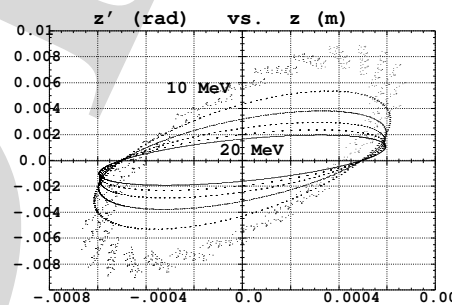


Figure 6: Vertical motion on about $\beta\gamma\epsilon_z = 10\pi$ mm.mrad invariant, horizontal motion launched on closed orbit. Note : the inward, spiral motion on 10 MeV is independent of the integration step size.

Tunes in the latter case are given in Fig. 4, together with regular resonance lines up to 5th order. Fig. 5 illustrates the reason for the decrease in the horizontal (when comparing Fig. 3-left and Fig. 3-right) in two cases, 10 and 16 MeV. The straddling of a sum resonance, or the vicinity of resonance nodes may also be a cause of horizontal DA decrease particle loss - this is to be investigated further.

Fig. 6 shows typical vertical motion at large amplitude.

3 Longitudinal motion

3.1 Time of flight

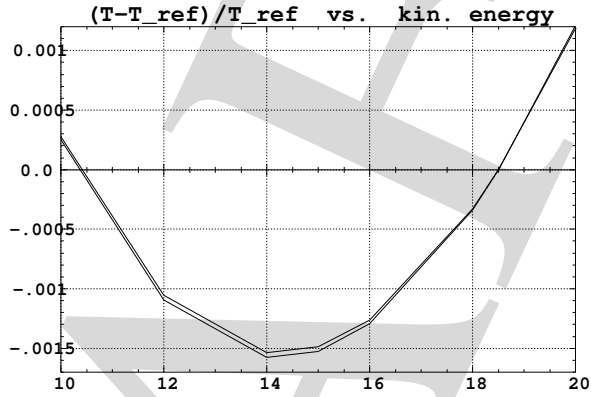


Figure 7: $(T - T_{Ref})/T_{Ref}$ as a function of energy. T_{Ref} is for 18.5 MeV kinetic energy (19.011 MeV/c). The lower curve corresponds to magnets with fringe fields, the upper one to sharp edge magnets.

Fig. 7 displays the relative time of flight difference (the so called “time of flight parabola”), with reference kinetic energy 18.5 MeV. The second zero in $(T - T_{Ref})/T_{Ref}$ is close to 10.5 MeV kinetic energy.

3.2 Serpentine

The 3 plots in Fig. 8 show the shape of the portrait in E-Phase space depending on the RF frequency, for a few particles launched around $E_{initial} = 10$ MeV.

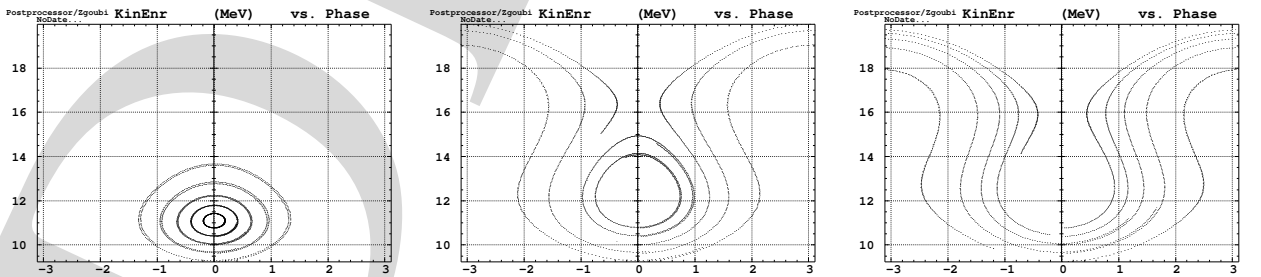


Figure 8: From left to right : $f_{RF} = 1.3504, 1.3512, 1.3514$ GHz. The central frequency is that used in the next Section “Acceleration” (see App. A). Fringe field set.

3.3 More serpentine

Acceleration of elliptical rings, zero transverse emittance. $f_{RF} = 1.3515$ GHz, $\hat{V} = 60$ kV/cavity.

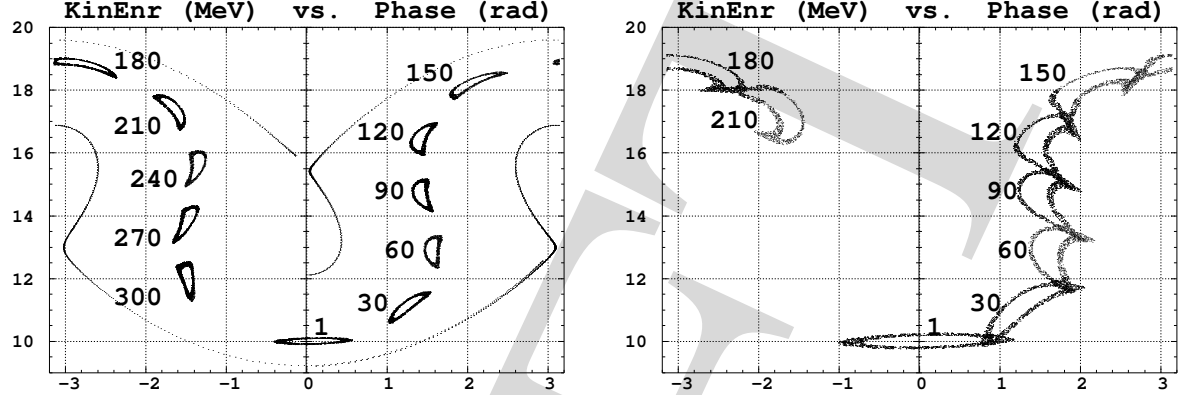


Figure 9: Acceleration of elliptical rings. The number of cavity passes is given next to each bunch projection. Left : longitudinal emittance $\epsilon_l/\pi \approx 0.06 10^{-4}$ eV.s, initial dimensions ± 0.11 MeV, ± 0.06 ns. The limits of the serpentine channel stem from two particular trajectories. Right : $\epsilon_l/\pi \approx 0.3 10^{-4}$ π eV.s, other conditions identical to the left plot ones.

3.4 6-D acceleration

Working hypothesis : one cavity every 3 other cell, 60 kV per cavity, $f_{RF} = 1.35$ GHz. The top energy is attained in about 220 pass in the cavities. Data details in App. A.

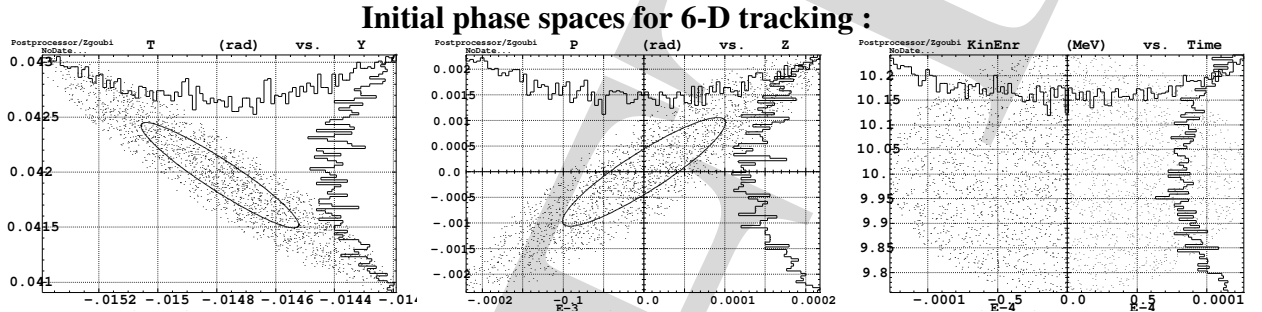


Figure 10: The 2000 particle bunch launched for acceleration (see Fig. 11) has initial $\epsilon_x = \epsilon_z \approx 5 10^{-8} \pi \text{ m.rad}$, and $\epsilon_l \approx 0.3 10^{-4} \pi \text{ eV.s.}$

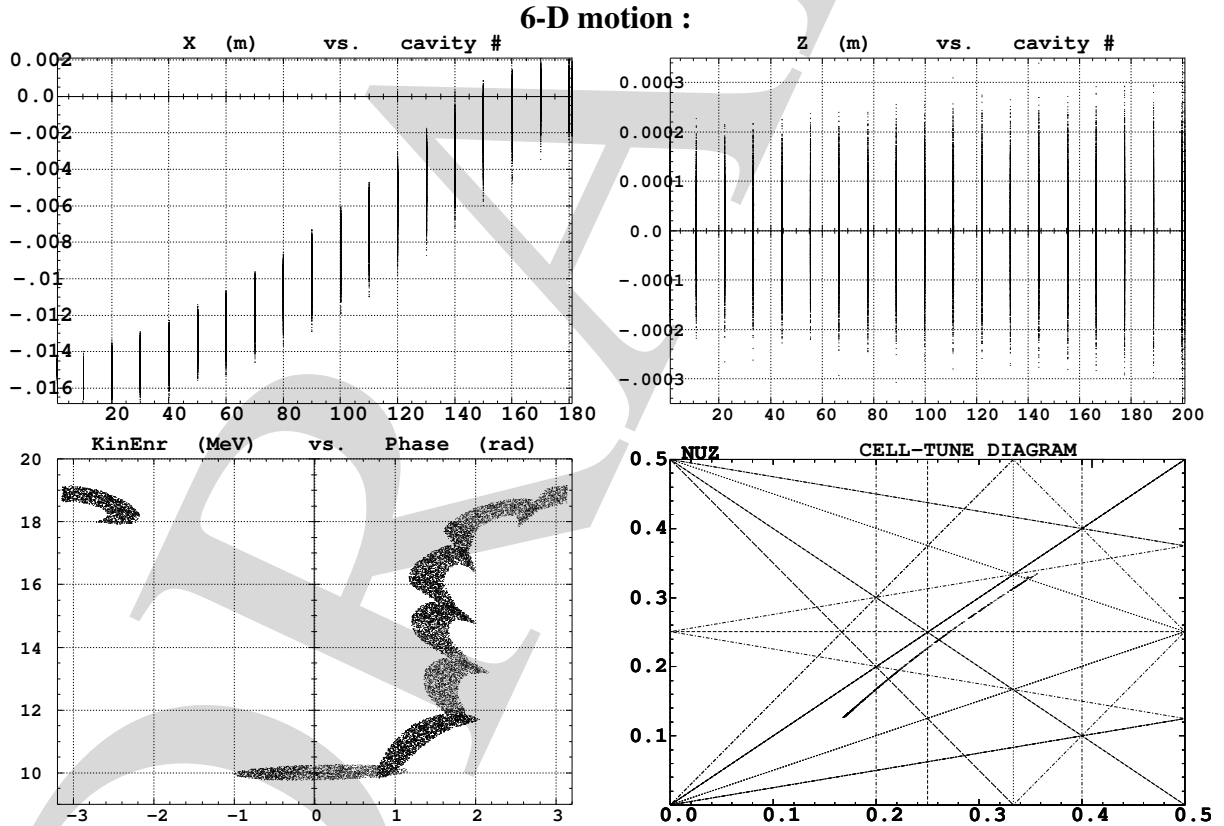


Figure 11: A 2000 particle bunch with initial conditions of Fig. 10 is accelerated. Fringe fields set. Top, left and right : resp. x-s and z-s every 10 other cavity. Right : longitudinal. Bottom, left : longitudinal phase-space ; bottom, right : beam path in the cell-tune diagram, from injection energy (larger tunes) to top energy (lower tunes) - resonance lines up to 6th order are shown.

APPENDIX

A Zgoubi data file

```

Carol/Shane/Scott's cell, PAC05%          10:1758, 12:830
'MCOBJET'
63.4138733   19.011MeV/c
3
2000
3 3 3 3 2 2
-1.47928846E-02  4.19796453E-2 0. 0. 0. 0.55223661 '0'
1.236454  0.729203  .5e-6 4      5e-8 pi.m.rad
-0.964399  0.100326  .5e-6 4
0. 3 1E-3 .7           0.3e-4 pi.eVs
123456 234567 345678
'PARTICUL'
0.5109989  1.60217733D-19 0. 0. 0.
'FAISCEAU'
'MULTIPOLE QUAD      QFD
0 .Quad
    3.0000 10.00  0.0  7.17210871262145 0.0 0.0 0.0 0.0
0. 0. 0. 0. 0. 0. 0. 0. 0.
4 .1455  2.2670  -.6395  1.1558  0. 0. 0.
2 1.1  1.00 1.00 1.00 1.00 1. 1. 1. 1.
4 .1455  2.2670  -.6395  1.1558  0. 0. 0.
0. 0. 0. 0. 0. 0. 0. 0.
0.05 #10|10|10 Quad QFD
1 0. 0.
'FAISCEAU'
'DRIFT'   DRIF     DMD
    4.006526
'CHANGREF'
0. 0. -4.2851836
'CHANGREF'
0 8.82393E-2 0.
'FAISCEAU'
'MULTIPOLE RBEN     DD
0 .Dip
    6.9984 10.00 +1.353978414314032 -5.443446612656280 0.0000
2 1.1  1.00 1.00 1.00 1.00 1. 1. 1. 1.
4 .1455  2.2670  -.6395  1.1558  0. 0. 0.
2 1.1  1.00 1.00 1.00 1.00 1. 1. 1. 1.
4 .1455  2.2670  -.6395  1.1558  0. 0. 0.
0. 0. 0. 0. 0. 0. 0. 0.
0.05 #10|10|10 Dip DD
1 0. 0.
-0.0747998250854
'FAISCEAU'
'CHANGREF'
0 -8.811538e-2 0.
'CHANGREF'
0 0. -4.28309007374 -4.285714285714285714037896646289027557941
'DRIFT'   DRIF     RFDD
    20.0000
'FAISCEAU'
'MULTIPOLE QUAD      QFD
0 .Quad
    3.0000 10.00  0.00000 7.17210871262145 0.0 0.0 0.0 0.0 0.0
2 1.1  1.00 1.00 1.00 1.00 1. 1. 1. 1.
4 .1455  2.2670  -.6395  1.1558  0. 0. 0.
0. 0. 0. 0. 0. 0. 0. 0.
4 .1455  2.2670  -.6395  1.1558  0. 0. 0.
0. 0. 0. 0. 0. 0. 0. 0.
0.05 #10|10|10 Quad QFD
0 0. 0. 0. 0. 0. 0. 0.
'FAISCEAU'      'END'
'CAVITE'
7
1.106565113  1.3515e9 ORBIT LENGTH at 19.011MeV, freq
60e3  0. VLT, Phi_0
'FAISTORE'
b_zgoubi.fai
10
'REBELOTE'
180  0.2  99      3700  0.1  99
'END'
7
'FAISCEAU'
'MULTIPOLE QUAD      QFD
0 .Quad
    3.0000 10.00  0.00000 7.17210871262145 0.0 0.0 0.0 0.0 0.0
2 1.1  1.00 1.00 1.00 1.00 1. 1. 1. 1.
4 .1455  2.2670  -.6395  1.1558  0. 0. 0.
2 1.1  1.00 1.00 1.00 1.00 1. 1. 1. 1.
4 .1455  2.2670  -.6395  1.1558  0. 0. 0.
0. 0. 0. 0. 0. 0. 0. 0.
0.05 #10|10|10 Quad QFD
1 0. 0.
'FAISCEAU'
'DRIFT'   DRIF     DMD
    4.006526
'CHANGREF'
0. 0. -4.2851836
'CHANGREF'
0 8.82393E-2 0.
'FAISCEAU'
'MULTIPOLE RBEN     DD
0 .Dip
    6.9984 10.00 +1.353978414314032 -5.443446612656280 0.0000
2 1.1  1.00 1.00 1.00 1.00 1. 1. 1. 1.
4 .1455  2.2670  -.6395  1.1558  0. 0. 0.
2 1.1  1.00 1.00 1.00 1.00 1. 1. 1. 1.
4 .1455  2.2670  -.6395  1.1558  0. 0. 0.
0. 0. 0. 0. 0. 0. 0. 0.
0.05 #10|10|10 Dip DD
1 0. 0.
-0.0747998250854
'FAISCEAU'
'CHANGREF'
0 -8.811538e-2 0.
'CHANGREF'
0 0. -4.28309007374 -4.285714285714285714037896646289027557941
'DRIFT'   DRIF     RFDD
    20.0000
'FAISCEAU'
'MULTIPOLE QUAD      QFD
0 .Quad
    6.0000 10.00  0.00000 7.17210871262145 0.0 0.0 0.0 0.0 0.0
2 1.1  1.00 1.00 1.00 1.00 1. 1. 1. 1.
4 .1455  2.2670  -.6395  1.1558  0. 0. 0.
2 1.1  1.00 1.00 1.00 1.00 1. 1. 1. 1.
4 .1455  2.2670  -.6395  1.1558  0. 0. 0.
0. 0. 0. 0. 0. 0. 0. 0.
0.05 #10|10|10 Quad QFD
1 0. 0.
'FAISCEAU'
'DRIFT'   DRIF     DMD
    4.006526
'CHANGREF'
0. 0. -4.2851836
'CHANGREF'
0 8.82393E-2 0.
'FAISCEAU'
'MULTIPOLE RBEN     DD
0 .Dip
    6.9984 10.00 +1.353978414314032 -5.443446612656280 0.0000
2 1.1  1.00 1.00 1.00 1.00 1. 1. 1. 1.
4 .1455  2.2670  -.6395  1.1558  0. 0. 0.
2 1.1  1.00 1.00 1.00 1.00 1. 1. 1. 1.
4 .1455  2.2670  -.6395  1.1558  0. 0. 0.
0. 0. 0. 0. 0. 0. 0. 0.
0.05 #10|10|10 Dip DD
1 0. 0.
-0.0747998250854
'FAISCEAU'
'CHANGREF'
0 -8.811538e-2 0.
'CHANGREF'
0 0. -4.28309007374 -4.285714285714285714037896646289027557941
'DRIFT'   DRIF     RFDD
    20.0000
'FAISCEAU'
'MULTIPOLE QUAD      QFD
0 .Quad
    6.0000 10.00  0.00000 7.17210871262145 0.0 0.0 0.0 0.0 0.0

```